

- Hildebrand and G. T. Penfield, *Eos* 71, 1425 (1990).
5. F. J.-M. R. Maurrasse, *Geol. Soc. Am. Abstr. Progr.* 22, 77 (1990).
 6. ———, F. Pierrelouis, J. J.-G. Rigaud, *Transactions of the Fourth Latin American Geological Congress* (Ministry of Energy and Natural Resources, Port-of-Spain, Trinidad, 1979/1985), p. 328.
 7. F. J.-M. R. Maurrasse, Ed., *Transactions du 1er Colloque sur la Geologie d'Haiti*, Port-au-Prince, 27 to 29 Mars 1980 (Imprimerie La Natal, Port-au-Prince, 1982), p. 184; *ibid.*, p. 246; *Survey of the Geology of Haiti: Guide to the Field Excursions in Haiti* (Miami Geological Society, Miami, 1982).
 8. The Beloc Formation overlies the ophiolite complex of the Dumisseau Formation; for details see F. Maurrasse, J. Husler, G. Georges, R. Schmitt, P. Damond, *Geol. Mijnb.* 58, 71 (1979).
 9. G. A. Izett, F. J.-M. R. Maurrasse, F. E. Lichte, G. P. Meeker, R. Bates, *U.S. Geol. Surv. Open-File Rep. OF-90-635* (1990).
 10. Rock-Color Chart, distributed by the Geological Society of America, 1979 edition.
 11. X-Ray diffraction of the insoluble residues indicates the presence of clinoptilolite and smectite from the alteration of mafic materials of these tektites. Also, see discussion by Izett *et al.* (9). For more detailed description of the basement rocks, see (8, 12).
 12. G. Sen and F. Maurrasse, Eds., *Transactions Eleventh Caribbean Geological Conference* (Caribbean Geological Congress, Bridgetown, Barbados, 1986), chap. 25; G. Sen, R. Hickey-Vargas, D. G. Waggoner, F. Maurrasse, *Earth Planet. Sci. Lett.* 87, 423 (1988).
 13. Also see W. Alvarez, L. W. Alvarez, F. Asaro, H. V. Michel, *Geol. Soc. Am. Spec. Pap.* 190, 305 (1982); C. Jehanno *et al.*, *Lunar Planet. Sci. XXII*, 641 (1991).
 14. D. Johnson, *J. Geomorph.* 2, 213 (1939); P. H. Kuenen and C. I. Migliorini, *J. Geol.* 58, 91 (1950); A. H. Bouma, *Sedimentology of Some Flysch Deposits: A Graphic Approach to Facies Interpretation* (Elsevier, Amsterdam, 1962), p. 168; R. G. Walker, *Proc. Yorkshire Geol. Soc.* 35, 1 (1965); G. M. Friedman and J. E. Sanders, *Principles of Sedimentology* (Wiley, New York, 1978).
 15. H. Sigurdsson *et al.*, *Nature* 349, 482 (1991).
 16. F. J.-M. R. Maurrasse, Ed. [*Transactions du 1er Colloque sur la Geologie d'Haiti*, Port-au-Prince, 27 to 29 Mars 1980 (Imprimerie La Natal, Port-au-Prince, 1982), p. 184] indicated the presence of clino- and orthopyroxene, spinel, and possibly some microtektites within the upper part of the marker bed where calcareous components are predominant.
 17. The origin of glassy microspherules is discussed in J. A. O'Keefe, *Tektites* (Univ. of Chicago Press, Chicago, 1963).
 18. Sigurdsson *et al.* (15) reported (p. 482) that amber to yellowish glasses are more vesicular than the deep brown glasses (cited as black glasses).
 19. Sigurdsson *et al.* (15) calculated the composition of a target rock as a mixture of argillaceous sediments and calcite. They used a MgO-rich argillite for comparison with their postulated impact rock, which explains why they noted that the MgO value of the calculated target rock was too high.
 20. N. T. Edgar *et al.*, *Initial Rep. Deep Sea Drill. Proj.* 15, 1137 (1973); I. Premoli-Silva and H. Bolli, *ibid.*, p. 499; F. Maurrasse, *ibid.*, p. 833; M. A. Gamper, *Rev. Inst. Geol. Univ. Autonoma Mexico* 1, 23 (1977); F. J.-M. R. Maurrasse, G. Fernandez, F. Quintas, J. R. Sanchez, J. L. Cobiella, in preparation.
 21. J. Hofker, *J. Foraminiferal Res.* 8, 46 (1978); G. Keller, *Mar. Micropaleontol.* 13, 239 (1988); in *Global Catastrophes in Earth History: An Interdisciplinary Conference on Impacts, Volcanism, and Mass Mortality* (Lunar and Planetary Institute, Houston, 1988), pp. 88–91; *Paleoceanography* 4, 287 (1989).
 22. See (6, 7) for a discussion of the biostratigraphy at Beloc.
 23. Uncertainty associated with the identification of certain species seems to have also led to uncertainties in the true range of taxa at the Cretaceous-Tertiary boundary. Comparative studies of specimens from different sections and isotopic investigations may help identify areas of stratigraphic continuity; see, for example, E. A. Pessagno, J. J. F. Longoria, H. Montgomery, C. C. Smith, *Geol. Soc. Am. Abstr. Progr.* 22, 277 (1990); J. Bourgeois, *Geol. Soc. Am. Bull.* 103, 434 (1991); G. Keller, *ibid.*, p. 435.
 24. Besides diagenesis, which may have affected the nannoflora, Coccolithophorids give conflicting evidence at Beloc because Maastrichtian forms predominate within the boundary level identified as Tertiary on the basis of the planktonic foraminifera [see (7) for details]. Similar observations have been reported by M. J. Jiang and S. Gartner [*Micropaleontology*, 32, 232 (1986)].
 25. Maurrasse and others (6, 7) originally interpreted materials of the boundary bed as volcanogenic, because they are reminiscent of altered vesicles in a palagonitic matrix similar to the underlying Dumisseau Formation basalts [for details of these basalts see (8, 12)].
 26. For a recent review of the debate, see G. A. Izett, *Geol. Soc. Am. Spec. Pap.* 249 (1990).
 27. J. Bourgeois, T. A. Hansen, P. L. Wiberg, E. G. Kauffman, *Science* 241, 567 (1988); J. Bourgeois, P. L. Wiberg, T. Hansen, in *Global Catastrophes in Earth History: An Interdisciplinary Conference on Impacts, Volcanism, and Mass Mortality* (Lunar and Planetary Institute, Houston, 1988), pp. 21–22.
 28. See D. Bukry, R. Douglas, S. A. Kling, V. Krashennnikov, *Initial Rep. Deep Sea Drill. Proj.* 6, 1253 (1971); J. A. McGowan, *ibid.* 22, 609 (1974).
 29. The excellent preservation of the planktonic foraminifera indicates that the deposit accumulated above the existing lysocline; W. H. Berger, *Mar. Geol.* 8, 111 (1970).
 30. T. J. Ahrens and J. D. O'Keefe, *Proc. Lunar Planet. Sci. Conf.* 13, A799 (1983).
 31. A 30-m thick polymictic megabreccia is intercalated in pelagic sediments of the Beloc formation at the K-T boundary at another locality southeast of Beloc.
 32. Serpentinic megabreccia of the Picota Formation is associated with the K-T boundary in the deep-water deposits of the Micara Formation, southern Cuba; J. L. Cobiella, *Mineria Cuba* 4, 46 (1978); ———, F. Quintas, M. Campos, M. H. Hernandez, *Geologia de la Region Central y Suroriental de la Provincia de Guantamano* (Editorial Oriente, Santiago de Cuba, 1984).
 33. K. G. Caldeira and M. R. Rampino, in *Global Catastrophes in Earth History: An Interdisciplinary Conference on Impacts, Volcanism, and Mass Mortality* (Lunar and Planetary Institute, Houston, 1988), p. 23; B. R. T. Simoneit and P. A. Meyers, *Geol. Soc. Am. Abstr. Progr.* 22, 278 (1990); M.-P. Aubry, *ibid.*, p. 107; A. Boersma and I. Premoli-Silva, *ibid.*, p. 106.
 34. Giant submarine collapses, like those that have occurred in sub-recent times in the Pacific, might also be a mechanism for the subsequent disturbance; P. W. Lipman, W. R. Normark, J. G. Moore, J. B. Wilson, C. E. Gutmacher, *J. Geophys. Res.* 93, 4279 (1988); J. G. Moore *et al.*, *ibid.* 94, 17465 (1989).
 35. R. S. Carmichael, *Practical Handbook of Physical Properties of Rocks and Minerals* (CRC Press, Boca Raton, FL, 1989).
 36. T. W. Donnelly, *Bull. Volcanol.* 43, 347 (1980).
 37. We thank G. Izett for the initial information about the glasses, R. Bates for encouraging discussions, G. Draper for comments on an earlier version of the manuscript, and J. R. Sanchez, J. L. Cobiella, M. Campos-Dueñas, and R. Guardado Lacaba for the opportunity to do fieldwork (F.M.) on the K-T section in Cuba. We also thank the Haitian Bureau of Mines and Energy Resources for logistic support of our field work in Haiti. Supported in part by Florida International University and the National Science Foundation (EAR76-22620 to F.M.; EAR-8815858 and EAR-8903879 to G.S.)

8 January 1991; accepted 28 March 1991

Identification of Widespread Pollution in the Southern Hemisphere Deduced from Satellite Analyses

J. FISHMAN,* K. FAKHRUZZAMAN, B. CROS, D. NGANGA

Vertical profiles of ozone obtained from ozonesondes in Brazzaville, Congo (4°S, 15°E), and Ascension Island (8°S, 15°W) show that large quantities of tropospheric ozone are present over southern Africa and the adjacent eastern tropical South Atlantic Ocean. The origin of this pollution is widespread biomass burning in Africa. These measurements support satellite-derived tropospheric ozone data that demonstrate that ozone originating from this region is transported throughout most of the Southern Hemisphere. Seasonally high levels of carbon monoxide and methane observed at middle- and high-latitude stations in Africa, Australia, and Antarctica likely reflect the effects of this distant biomass burning. These data suggest that even the most remote regions on this planet may be significantly more polluted than previously believed.

WIDESPREAD AIR POLLUTION HAS generally been regarded as an anthropogenic phenomenon identifiable with industrialized nations, primarily in the Northern Hemisphere. Recent satellite measurements of ozone (O₃) in the

troposphere (1) define distinct plumes emanating from North America, Asia, and Europe. When these data are compared with available ozonesonde measurements at sites with enough data to derive a climatology of free tropospheric O₃, the differences in agreement between the satellite analysis and the ozonesonde measurements are generally smaller than 15% (1). The satellite measurements also indicate that a large amount of O₃ pollution comes from tropical southern Africa and that this source is most pronounced during the dry season from August to October. In addition, elevated concentrations of carbon monoxide (CO) and meth-

J. Fishman, Atmospheric Sciences Division (Mail Stop 401A), National Aeronautics and Space Administration, Langley Research Center, Hampton, VA 23665.
K. Fakhruzzaman, ST Systems Corporation, Hampton, VA 23666.
B. Cros and D. Nganga, Laboratoire de Physique de l'Atmosphere, Universite Maïen Ngouabi, Brazzaville, Republic of Congo.

*To whom correspondence should be addressed.

ane (CH_4) have been observed on a seasonal basis in the Southern Hemisphere. Both CH_4 and CO are trace gases that would be present in the atmosphere even without sources from anthropogenic activity. Because industrialization is less in the Southern Hemisphere than in the Northern Hemisphere, it has generally been assumed that the concentrations of both of these trace gases in the remote regions of this hemisphere are not greatly influenced by pollution. But the source of the seasonality of these trace gases has been unclear. In this report, we compare the data from satellite and in situ measurements to investigate the origin of these trace gases, and we suggest that pollution originating from biomass burning in tropical and subtropical southern Africa has a pronounced influence on the seasonal cycles of CO and CH_4 that have been observed throughout the Southern Hemisphere.

More than 32,000 concurrent satellite measurements have been made from the Total Ozone Mapping Spectrometer (TOMS) and the Stratospheric Aerosol Gas Experiments (SAGE) between 1979 and 1989 (Fig. 1) (2). Tropospheric O_3 levels can be obtained by subtracting the amount of O_3 in the stratosphere, derived from the SAGE measurements, from the concurrent

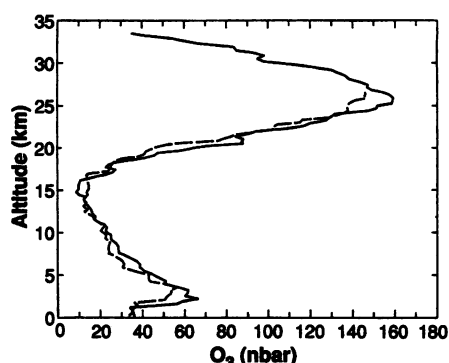


Fig. 2. Ozonesondes from Brazzaville (solid line) and Ascension Island (dashed line) for 6 and 7 August 1990, respectively.

measurement of total O_3 measured by TOMS at the same location. The difference is approximately 10% of the total signal and is referred to as the tropospheric residual (1).

The tropospheric data show a well-defined maximum in O_3 of greater than 45 Dobson units [1 Dobson unit (D.U.) = 2.69×10^{16} molecules of O_3 per square centimeter] off the west coast of southern Africa during September and October. To investigate the origin of these elevated O_3 concentrations, we used ozonesondes (3) at Brazzaville, Congo (4°S, 15°E), and at As-

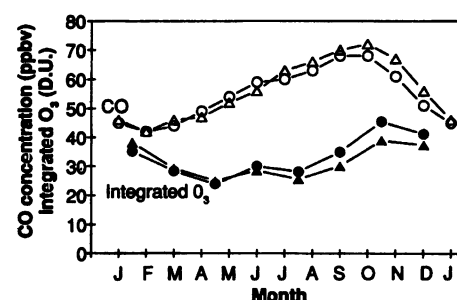


Fig. 3. The seasonal cycles of CO at Cape Point, Africa (○), and Cape Grim, Australia (△), and the integrated amount of O_3 at the same two locations (● and ▲). Data derived from the satellite technique used to construct Fig. 1.

cension Island (8°S, 15°W) to obtain more accurate O_3 measurements (Fig. 2). Partial pressures of O_3 greater than 50 nbar were found between 1.5 and 4.3 km in the Brazzaville sounding. The O_3 concentration peaks at 66 nbar at an altitude of 2.2 km. The tropospheric O_3 distribution was generally similar at both localities, but the concentrations in the polluted layer at Ascension Island, where the highest tropospheric O_3 partial pressure was 56 nbar at 3.5 km, were typically 15 to 20% less than the concentrations in Brazzaville. These profiles substantiate our conclusion from satellite data that widespread air pollution is the reason for the enhancement observed over the western part of southern Africa. During the 1990 dry season, the average integrated amount of O_3 in the troposphere was 45 D.U., and the level at Brazzaville was ~8 D.U. higher than at Ascension Island.

The distribution of O_3 in the lower troposphere at Ascension Island supports the premise that the O_3 produced over southern Africa is transported by low-level easterlies to the eastern South Atlantic Ocean. Some of the O_3 in the boundary layer makes its way into the middle and upper troposphere, where the winds in the tropics and in the subtropics are generally westerlies (4). Because O_3 is long-lived in the free troposphere, it can be transported long distances. The satellite data for July-August and October-September (Fig. 1) show the long-range transport of this O_3 . The prevailing meteorology during November and December suggests that O_3 from both southern Africa and southeastern Brazil should feed into the region of elevated O_3 (>40 D.U.) over the South Atlantic Ocean near 25° to 30°S.

Examination of the annual cycles of CO and CH_4 at four locations in the Southern Hemisphere [Cape Point, South Africa (34°S, 18°E), Cape Grim, Australia (41°S, 145°W), Mawson, Antarctica (68°S, 63°E), and the South Pole] shows that the concentrations of these trace gases also exhibit a

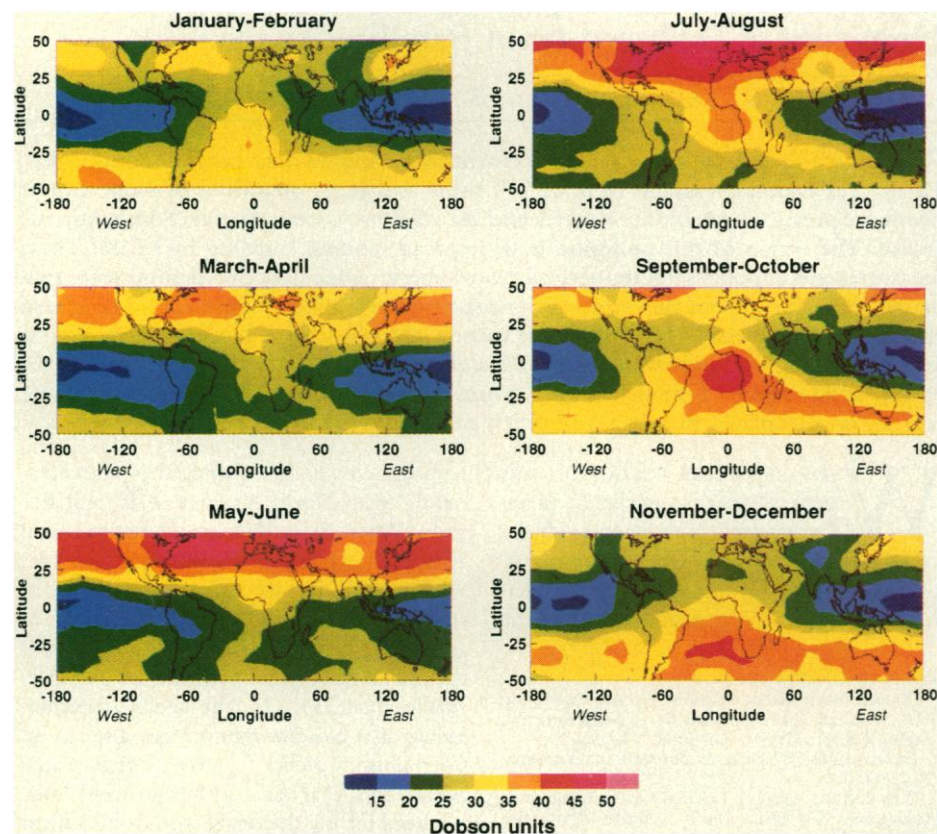


Fig. 1. Distribution of the tropospheric O_3 residual derived from data between 1979 and 1989 for bimonthly periods.

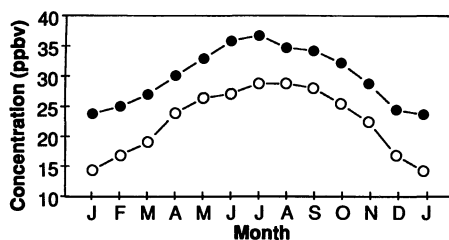


Fig. 4. The seasonal cycles of surface tropospheric O_3 for Cape Point ($34^\circ S$) (●) and Cape Grim ($41^\circ S$) (○).

distinct maximum during September and October (5, 6). Comparison of the seasonal cycles of CO and integrated O_3 in the troposphere at Cape Grim and Cape Point (Fig. 3) shows that both were enhanced during austral spring, September to November. The CO data are monthly averages; the O_3 data have been averaged over 45-day periods for 10° latitude by 20° longitude boxes centered on Cape Grim and Cape Point. The orbit of the satellites that carry the SAGE instruments is such that the same approximate location is sampled at intervals of ~ 40 days. Therefore, meaningful monthly averages cannot be obtained for every month.

The detrended CH_4 seasonal cycle at Cape Point and Cape Grim (7) is virtually identical to the seasonal cycle of CO; both have an amplitude of ~ 30 ppbv by volume (ppbv); the highest concentrations were in September to October and the lowest concentrations were in February. In contrast, in the Northern Hemisphere, the seasonal cycles of CH_4 and CO are quite different (8). Because the atmospheric lifetime of CH_4 is on the order of a decade, its seasonal cycle most likely reflects the seasonal variation of its sources rather than the seasonality of its removal mechanism, which is reaction with the hydroxyl (OH) radical. The primary sources of CH_4 are biomass burning, rice paddies and marshes, and enteric fermentation from ruminants (9). Each of these sources is estimated to release on the order of 1×10^{14} g of CH_4 per year. Only biomass burning is significantly concentrated in southern low latitudes.

In contrast to the cycle of CH_4 , the seasonal cycle of CO at these two sites partially reflects the seasonal nature of its removal by the OH radical. The atmospheric residence time of CO is 1 to 2 months, and the lowest OH concentrations at southern mid-latitudes are June and July. Therefore, the highest CO concentrations at southern mid-latitudes should occur in July or August, rather than October as observed. Results from a three-dimensional photochemical transport model (10) show that biomass burning, rather than the seasonal

variation of the OH radical at southern mid-latitudes, is the primary reason why the maximum observed at Cape Point and at Cape Grim occurs in October. Without seasonal input from biomass burning, the model yields a seasonal CO cycle that peaks in August and an average CO concentration in the Southern Hemisphere of only ~ 35 ppbv, lower by nearly a factor of 2 than the observations (Fig. 3). The amplitude of the CO seasonal cycle without biomass burning is only ~ 11 ppbv instead of the observed ~ 30 ppbv.

Satellite measurements of CO from two Space Shuttle flights in November 1981 and October 1984 (11) confirmed that large amounts of CO were coming from Africa as a result of widespread biomass burning. Subsequent analysis (4) of these data showed that CO over the eastern Indian Ocean was transported more than 7500 km to the southeast (almost to Australia). We propose that such long-range transport is not an occasional occurrence, but a common one that leads to the widespread dissemination of CO, CH_4 , and tropospheric O_3 from biomass burning. The seasonal cycle of elemental carbon (C) at Cape Grim also maximizes in October and supports this premise (12).

At both Cape Point and Cape Grim (Fig. 4), the highest concentration of surface O_3 (13) is found in July and the lowest concentration in January. This pattern is significantly different from the seasonal cycles of CO and CH_4 at the surface and the seasonal cycle of the satellite-derived tropospheric O_3 . To explain this apparent discrepancy, we compared the satellite-derived tropospheric O_3 data with the seasonal cycle of O_3 (at 500 mbar) derived from an analysis of 752 ozonesondes at Aspendale, Australia ($38^\circ S$, $145^\circ E$), between 1965 and 1982 (Fig. 5) (14). The satellite observations are in good agreement with the free tropospheric O_3 measurements. Earlier workers had assumed that middle tropospheric O_3 reached its highest concentrations in austral

spring, because this was when stratosphere-troposphere exchange was most intense (15). The spatial continuity provided by the satellite analysis, on the other hand, clearly shows that the excess O_3 at southern middle latitudes at this time of the year is transported from lower latitudes, not higher latitudes, and is thus from biomass burning, not the stratosphere.

We propose that the observed differences between the seasonal behavior of surface O_3 and the other trace species are related to the relatively short atmospheric residence time of surface O_3 compared to those of these other gases. The dominant sink for both CO and CH_4 is reaction with OH. If we assume that these two trace gases originate in the southern tropical and subtropical regions of the Southern Hemisphere, then the atmospheric residence time of these trace gases can be obtained if the OH concentration is known. Using the model-derived OH distribution computed in (10), we determined the atmospheric lifetime of CO to be approximately 30 days in the boundary layer and 40 days in the middle troposphere at these latitudes. For CH_4 , the atmospheric lifetime is approximately 3 years in the boundary layer and 8 years in the middle troposphere. These lifetimes are sufficiently long that CO and CH_4 produced in these regions can be transported substantial distances.

Ozone, however, is a different story. The primary photochemical sink for tropospheric O_3 is the reaction of metastable atomic oxygen, $O(^1D)$, one of the products of O_3 photolysis, with water vapor. Thus, the lifetime of tropospheric O_3 is most dependent on the distribution of water vapor and the amount of ultraviolet radiation available. In the tropical boundary layer, both of these are abundant, and we compute (16) a lifetime of only 2 to 5 days in the tropical planetary boundary layer. In the middle troposphere, however, we compute an atmospheric lifetime of approximately 90 days. Thus, the O_3 that is so abundant in the lower atmosphere over Brazzaville and Ascension Island (Fig. 2) does not persist long enough to be transported long distances. If, however, the O_3 can get out of the planetary boundary layer, the lifetime is sufficiently long that it can be transported significant distances. The seasonal cycle of O_3 at the surface may thus be controlled directly by the strength of the sink at these latitudes.

The data do not rule out other factors that contribute to the seasonal variability of the trace gas measurements summarized in this report. The agreement between the seasonal cycles of the satellite-derived tropospheric O_3 data and the surface CO and CH_4 measurements is not perfect, and other sources, sinks, and transport mechanisms are likely

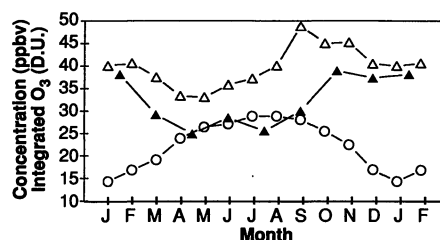


Fig. 5. The seasonal cycles of O_3 at 500 mbar (Δ) derived from ozonesonde data at Aspendale, Australia, between 1967 and 1982, and the tropospheric residual (from satellite data) (\blacktriangle) and surface O_3 measurements (\circ) at Cape Grim, Australia. Surface and 500-mbar data reported in parts per billion by volume, satellite data in D.U.

responsible for these observed differences in seasonal cycles. Nonetheless, we believe that the enhancement of trace gas concentrations in the Southern Hemisphere that is due to emissions from biomass burning in Africa and, to a lesser extent, South America, is the mechanism that determines much of the seasonality of these trace species.

REFERENCES AND NOTES

1. A climatology of tropospheric O_3 was developed from more than 22,000 satellite observations and compared with available tropospheric O_3 climatologies obtained from long-term ozonesonde records. This comparison was made for eight stations that operated during the same time over which the satellite measurements were made (1979 to 1987) and is described in J. Fishman *et al.*, *J. Geophys. Res.* **95**, 3599 (1990). The agreement between the satellite climatologies and the ozonesonde climatologies is better for stations at low latitudes, with differences of $\sim 10\%$.
2. TOMS was launched in October 1978 on Nimbus 7 and is still making measurements. SAGE was launched aboard the Atmospheric Explorer Mission 2 Satellite in February 1979 and operated through November 1981; SAGE II was launched aboard the Earth Radiation Budget Satellite in October 1984 and is still providing data.
3. Ozonesonde launches were initiated in early June 1990 at Brazzaville and in late July 1990 at Ascension Island. Because of technical difficulties, neither station has operated continuously through the dry season of 1990, and the only period of overlap was during early August 1990.
4. C. E. Watson, J. Fishman, H. G. Reichle, Jr., *J. Geophys. Res.* **95**, 16433 (1990).
5. The African measurements of CO and CH_4 discussed in this section were taken from H. E. Scheel, E.-G. Brunke, and W. Seiler [*J. Atmos. Chem.* **11**, 197 (1990)] and E.-G. Brunke, H. E. Scheel, and W. Seiler [*Atmos. Environ.* **24A**, 585 (1990)]. The Australian measurements were from B. W. Forgan and P. J. Fraser, Eds., *Baseline 86* (Australian Bureau of Meteorology, Aspendale, Australia 1986).
6. Additional information about the Antarctic stations has been taken from "Scientific Assessment of Stratospheric Ozone: 1989," *World Meteorological Organization Global Ozone Research Monitoring Project Report 20* (World Meteorological Organization, Geneva, 1989), vol. 1.
7. L. P. Steele *et al.* [*J. Atmos. Chem.* **5**, 127 (1987)] and M. A. K. Khalil and R. A. Rasmussen [*Environ. Sci. Technol.* **24**, 549 (1990)] showed that CH_4 is increasing at a rate of $\sim 1\%$ per year. The detrended seasonal cycle is what remains once this secular increase is removed from the data.
8. M. A. K. Khalil and R. A. Rasmussen, *J. Geophys. Res.* **88**, 5131 (1983); *Chemosphere* **20**, 227 (1990). Whereas CO seasonally displays a somewhat regular sinusoidal behavior at northern mid-latitudes, which is similar to (but 6 months out of phase with) the behavior in the Southern Hemisphere, the primary CH_4 sources are most pronounced at different times of the year, and within the hemisphere, different sources influence the seasonality at various locations.
9. M. A. K. Khalil and R. A. Rasmussen, *Tellus* **42B**, 229 (1990); P. J. Crutzen, I. Aselmann, W. Seiler, *ibid.* **38B**, 271 (1986); E. M. Matthews and I. Fung, *Glob. Biogeochem. Cycles* **1**, 61 (1987); R. J. Cicerone and J. D. Shetter, *J. Geophys. Res.* **86**, 7203 (1981); P. J. Crutzen *et al.*, *J. Atmos. Chem.* **2**, 233 (1985). Biomass burning is a highly seasonal phenomenon in both Africa and South America in the southern tropics, maximizing between August and October.
10. C. M. Spivakovsky *et al.*, *J. Geophys. Res.* **95**, 18441 (1990). Using this model, J. A. Logan *et al.* (in a paper presented at the 7th International Symposium of the Commission on Atmospheric Chemistry and Global Pollution, Chamrousse, France, September 1990) showed that a large source from tropical biomass burning, which is highly seasonal, must be present to account for the seasonal CO cycle observed in the Southern Hemisphere.
11. H. G. Reichle, Jr., *et al.*, *J. Geophys. Res.* **91**, 10865 (1986); H. G. Reichle, Jr., *et al.*, *ibid.* **95**, 9845 (1990).
12. J. Heintzenberg and E. K. Bigg, *Tellus* **42B**, 355 (1990).
13. The tropospheric O_3 data have been summarized in (5).
14. J. A. Logan, *J. Geophys. Res.* **90**, 10463 (1985).
15. J. Fishman, in *Ozone in the Free Atmosphere*, R. C. Whitten and S. S. Prasad, Eds. (Van Nostrand Reinhold, New York, 1985) pp. 161–194.
16. The photochemical lifetimes for O_3 have been derived with a modified numerical model described in J. Fishman and T. A. Carney, *J. Atmos. Chem.* **1**, 351 (1984); J. Fishman, F. M. Vukovich, E. V. Browell, *ibid.* **3**, 299 (1985); T. A. Carney and J. Fishman, *Tellus* **38B**, 127 (1986). The inputs for these calculations have been modified to be in reasonably good agreement with O_3 , water vapor, CO, and temperature measurements characteristic of those found during field missions in Brazil in 1985 and 1987, described by R. C. Harriss *et al.* [*J. Geophys. Res.* **93**, 1351 (1988)] and R. C. Harriss *et al.* [*ibid.* **95**, 16721 (1990)].
17. We thank G. Brothers for help in establishing ozonesonde sites and T. Owens, R. Bendura, R. Bull, and A. Torres for their assistance. The ozonesondes at Ascension Island were launched by G. Talbot in cooperation with the U.S. Air Force. We thank Cl. Bouka-Biona, A. Minga, and the Agency for the Security of Air Navigation crew for their assistance in Brazzaville. We have benefited from discussions with M. Fenn, C. P. Rinsland, R. C. Harriss, M. A. K. Khalil, C. M. Spivakovsky, J. A. Logan, and P. J. Crutzen. We thank M. A. K. Khalil and C. M. Spivakovsky for sharing some of their unpublished data with us. This work has been funded through NASA's Global Tropospheric Experiment.

19 December 1990; accepted 18 March 1991

Identity Elements for Specific Aminoacylation of Yeast tRNA^{Asp} by Cognate Aspartyl-tRNA Synthetase

JOERN PÜTZ, JOSEPH D. PUGLISI, CATHERINE FLORENTZ, RICHARD GIEGÉ*

The nucleotides crucial for the specific aminoacylation of yeast tRNA^{Asp} by its cognate synthetase have been identified. Steady-state aminoacylation kinetics of unmodified tRNA transcripts indicate that G34, U35, C36, and G73 are important determinants of tRNA^{Asp} identity. Mutations at these positions result in a large decrease (19- to 530-fold) of the kinetic specificity constant (ratio of the catalytic rate constant k_{cat} and the Michaelis constant K_m) for aspartylation relative to wild-type tRNA^{Asp}. Mutation to G10-C25 within the D-stem reduced k_{cat}/K_m eightfold. This fifth mutation probably indirectly affects the presentation of the highly conserved G10 nucleotide to the synthetase. A yeast tRNA^{Phe} was converted into an efficient substrate for aspartyl-tRNA synthetase through introduction of the five identity elements. The identity nucleotides are located in regions of tight interaction between tRNA and synthetase as shown in the crystal structure of the complex and suggest sites of base-specific contacts.

THE CORRECT AMINOACYLATION OF tRNAs by their cognate synthetase is crucial for accurate transmission of genetic information and is determined by certain structural features of the tRNA, which in certain systems include nucleotides in the anticodon loop, acceptor stem, and D-loop (1). Regions of contact between yeast tRNA^{Asp} and yeast aspartyl-tRNA synthetase (AspRS) have been previously characterized with chemical and enzymatic footprinting methods (2, 3). A high-resolution x-ray structure of this complex (4) has confirmed that the anticodon loop and stem as well as portions of the acceptor stem are sites of interaction with AspRS. We describe steady-state aminoacylation kinetics for a series of mutant transcripts of yeast tRNA^{Asp} in order to delineate the determi-

nant nucleotides important for aminoacylation by yeast AspRS.

The aminoacylation kinetics of mutant tRNAs were compared to that of the unmodified transcript of yeast tRNA^{Asp} in which U1-A72 base pair was changed to G1-C72 (Fig. 1A); both transcripts have equivalent kinetic parameters for aspartylation as the fully modified molecule (5). Since the transcript of *Escherichia coli* tRNA^{Asp} is an equivalent substrate for aspartylation by yeast AspRS as the yeast transcript (Table 1), a number of nucleotide positions could be eliminated as potential identity elements (Fig. 1B). Moreover, single-stranded nucleotides protected in footprinting experiments (2, 3), G-U base pairs (6), and nucleotides identified by computer sequence analysis (7) as specific for tRNA^{Asp} were tested explicitly. For simplicity, the effects of mutations (Fig. 1C) on the steady-state aminoacylation kinetics (Table 1) are described below in terms of the four structural domains of the tRNA molecule.

Laboratoire de Biochimie, Institut de Biologie Moléculaire et Cellulaire du CNRS, 15 rue René Descartes, F-67084 Strasbourg Cedex, France.

*To whom correspondence should be addressed.